

Real Exchange Rates and Endogenous Productivity: Online Appendix

Nils Gornemann and Pablo A. Guerrón Quintana and Felipe Saffie*

December 2, 2024

D Online Appendix: Additional Results

This appendix contains additional results for the estimated parameters of the various models as well as additional results from robustness checks of the full model.

D.1 Estimation

This subsection collects some additional results regarding the estimations performed in the paper. Table 9 collects the calibrated parameters for the simple model. Table 10 summarizes the calibrated parameters in the full model. Table 11 displays the estimated parameters for the shock processes from the full endogenous and exogenous growth models.

*Gornemann: Board of Governors, nilsgornemann@gmail.com. Guerrón Quintana: Boston College, pguerron@gmail.com. Saffie: University of Virginia, Darden School of Business, saffieF@darden.virginia.edu. The views in this paper are solely the responsibility of the authors and should not be interpreted as reflecting the views of the Board of Governors of the Federal Reserve System or any other person associated with the Federal Reserve System.

Table 9: Calibrated Parameters–Simple Model

Parameter	Value	Interpretation
σ	5	Risk Aversion
β	1.0151	Time Preference
ϕ_1	0.01	Bond Holding Cost
δ_k	0.015	Capital Depreciation
ϕ_i	0.1	Scale Investment Adjustment Cost
ρ	0.33	Elasticity Substitution Home and Foreign Good
a_D	0.9799	Scale Preference Home Good
a_I	0.0965	Scale Preference Foreign Good
α_K	0.2	Capital Share Production
α_L	0.3	Labor Share Production
α_M	0.5	Share Intermediate Goods Production
\bar{Z}	1.1802	Scale Production
Φ	0.0875	Fixed Cost Production
μ	0.625	Elasticity of Substitution Intermediate Goods
τ	0.1	Technology Cross-Country Spillover
η	0.5/0.25	Elasticity R&D Production
δ_a	0.025	Obsolescence of Adopted Products

Notes: This table lists the parameters that are calibrated to values shown here for the simple model. See the text for the details on the calibration targets. We omit scale parameters like ζ .

Table 10: Calibrated Parameters

Parameter	Value	Interpretation
σ	5	Risk Aversion
ϕ_1	0.01	Bond Holding Cost
δ_0	0.015	Capital Depreciation BGP
ρ	1.5	Elasticity Substitution Home and Foreign Good
ι	10	Trade Adjustment Cost
a_D	0.9820	Scale Preference Home Good
a_I	0.0898	Scale Preference Foreign Good
α_K	0.32	Capital Share Production
α_L	0.68	Labor Share Production
α_M	0.5	Share Intermediate Goods Production
\bar{Z}	2.375	Scale Production
Φ	0.258	Fixed Cost Production
μ	1.52	Elasticity of Substitution Intermediate Goods
δ_n	0.025	Obsolescence of New Ideas
δ_a	0.025	Obsolescence of Adopted Products
\bar{g}	0.106	Government Expenditure Share of Production

Notes: This table lists the parameters that are calibrated to values shown here in most of our exercises. See the text for the details on the calibration targets. We omit scale parameters like ψ_1 , as they depend on estimated parameters and are, therefore, varying across different exercises.

Table 11: Estimation Results - Main Specification - Shock Processes

Parameter	Endogenous Both Stages	Endogenous New Tech only	Exogenous
$100 * \sigma_{\psi_1}$	4.01 [2.91,5.13]	4.82 [3.57,6.07]	3.76 [2.70,4.82]
$100 * \sigma_{\psi_1}^*$	2.44 [1.78,3.10]	2.92 [2.18,3.63]	2.40 [1.73,3.07]
$100 * \sigma_Z$	0.20 [0.18,0.23]	0.21 [0.18,0.23]	0.23 [0.20,0.25]
$100 * \sigma_Z^*$	0.21 [0.19,0.23]	0.21 [0.19,0.23]	0.21 [0.19,0.23]
$100 * \sigma_\beta$	0.16 [0.07,0.24]	0.24 [0.08,0.42]	0.09 [0.07,0.10]
$100 * \sigma_\beta^*$	0.12 [0.07,0.17]	0.13 [0.08,0.18]	0.18 [0.11,0.24]
$100 * \sigma_g$	2.17 [1.97,2.35]	2.20 [1.99,2.41]	2.19 [1.99,2.39]
$100 * \sigma_g^*$	1.50 [1.35,1.65]	1.51 [1.37,1.65]	1.55 [1.41,1.69]
$100 * \sigma_q$	1.22 [0.90,1.53]	1.14 [0.81,1.46]	1.60 [1.01,2.17]
$100 * \sigma_q^*$	0.62 [0.48,0.76]	0.64 [0.46,0.78]	0.88 [0.58,1.17]
$100 * \sigma_{\Omega^g}$	3.44 [3.08,3.78]	3.45 [3.12,3.83]	3.46 [3.08,3.82]
$100 * \sigma_{\Omega^f}$	2.23 [1.99,2.48]	2.20 [1.96,2.43]	2.01 [1.79,2.22]
$100 * \sigma_\zeta$	1.24 [0.97,1.49]	1.57 [1.17,1.99]	
$100 * \sigma_\zeta^*$	1.39 [1.04,1.74]	1.62 [1.21,20.7]	
ρ_{ψ_1}	0.934 [0.922,0.947]	0.934 [0.922,0.945]	0.961 [0.949,0.972]
$\rho_{\psi_1}^*$	0.929 [0.684,0.954]	0.927 [0.681,0.949]	0.937 [0.911,0.964]
ρ_Z	0.926 [0.893,0.961]	0.940 [0.924,0.957]	0.904 [0.864,0.945]
ρ_Z^*	0.968 [0.960,0.977]	0.968 [0.959,0.977]	0.967 [0.955,0.979]
ρ_β	0.949 [0.904,0.985]	0.923 [0.857,0.984]	0.993 [0.990,0.996]
ρ_β^*	0.947 [0.920,0.974]	0.944 [0.920,0.971]	0.941 [0.912,0.968]
ρ_g	0.979 [0.971,0.987]	0.978 [0.970,0.986]	0.971 [0.963,0.979]
ρ_g^*	0.978 [0.969,0.986]	0.975 [0.965,0.986]	0.965 [0.952,0.978]
ρ_q	0.951 [0.927,0.975]	0.948 [0.922,0.973]	0.309 [0.131,0.483]
ρ_q^*	0.628 [0.387,0.893]	0.668 [0.509,0.957]	0.332 [0.134,0.534]
ρ_{Ω^g}	0.961 [0.947,0.976]	0.963 [0.947,0.980]	0.983 [0.976,0.990]
ρ_{Ω^f}	0.982 [0.972,0.992]	0.981 [0.972,0.991]	0.973 [0.959,0.987]
ρ_ζ	0.974 [0.962,0.991]	0.966 [0.952,0.979]	
ρ_ζ^*	0.682 [0.861,0.946]	0.896 [0.842,0.946]	
ρ_U	0.983 [0.973,0.994]	0.984 [0.975,0.993]	0.899 [0.856,0.942]
$100 * \sigma_U$	0.10 [0.08,0.13]	0.10 [0.08,0.12]	0.19 [0.11,0.27]

Notes: This table lists the posteriors used in the estimation. The table reports the posterior mean and the 90% credible set. Parameters with a (#) are absent in the comparison model without endogenous growth.

D.2 Extra Figures and Tables

In this subsection, we display the results from some additional experiments.

Figure 21 displays the autocorrelation function from the full endogenous growth model when we turn off the UIP shocks in the simulations. The main takeaway is that, if anything, the model without the UIP shocks shows more persistence in the RER than in the data, illustrating that the UIP shock matters more for fitting short-run changes in the RER in the model. Importantly, this is despite the relatively high estimated autocorrelation of the UIP shock indicating that this value is not driving our model's success at low frequencies.

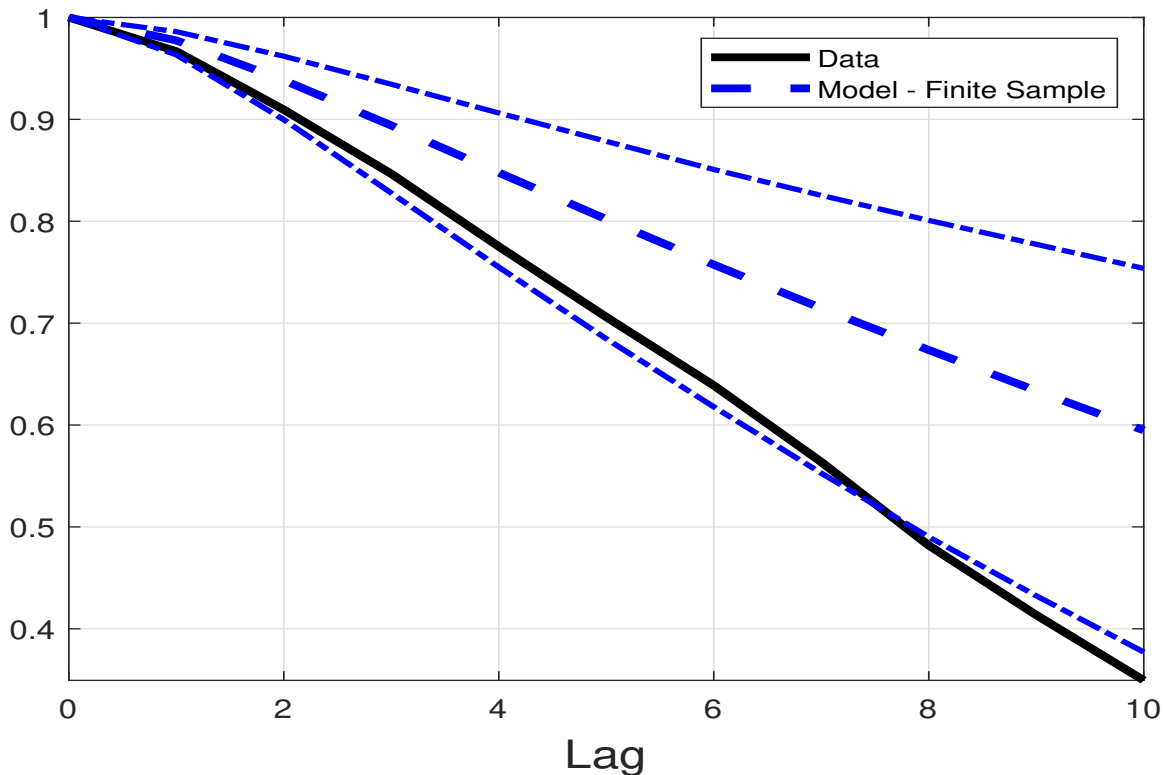


Figure 21: Autocorrelation – No UIP Shock

Notes: The thick blue broken line shows the median model autocorrelation simulated as described in the text, and the thinner blue lines the 68 percent bands from the simulations. The black line is the autocorrelation in the data.

In our baseline result, we simulated short samples from the posterior mean, but, alternatively, we can use the full potential of the Bayesian estimation and include parameter uncertainty by drawing a different parameter set for each simulation from the posterior distribution. Figure 22 shows that the endogenous model continues to successfully track the empirical spectrum while, even with the added parametric uncertainty, the exogenous growth credible sets cannot capture the empirical patterns.

The shocks used for the simulation on the model were not necessarily i.i.d. normal shocks, as they were bootstrapped from the empirically filtered innovations. Figure 23 shows that drawing from i.i.d. normal distributions with the posterior mode estimated variances does not change our

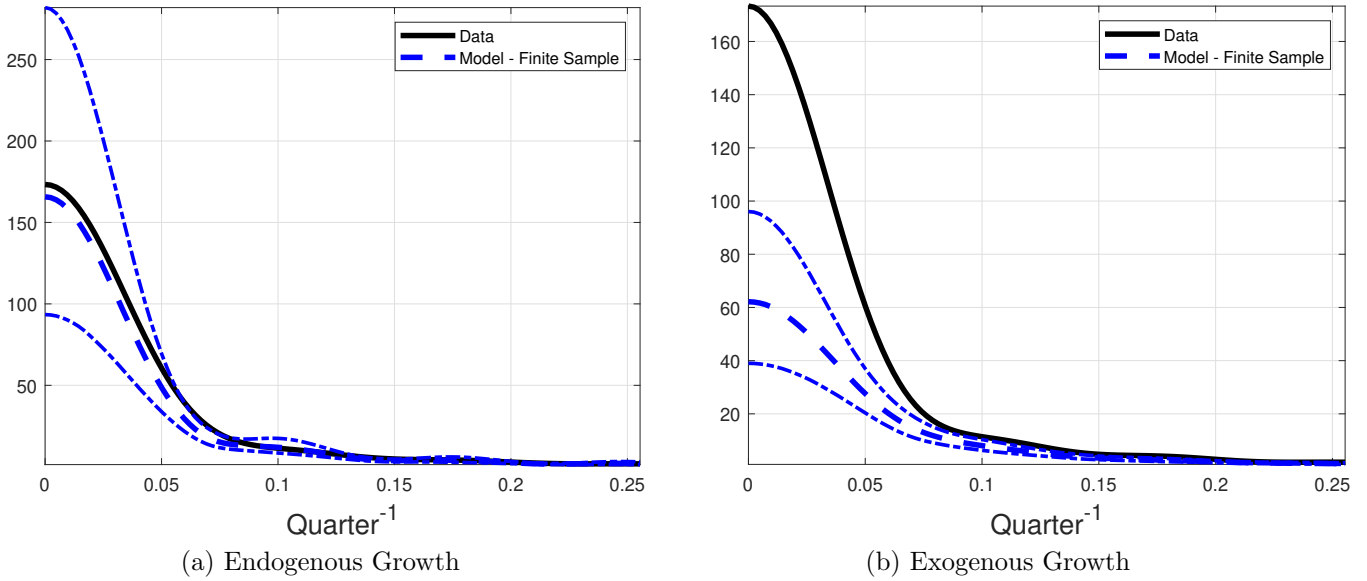


Figure 22: Robustness – Drawing of Posterior

Notes: The thick blue broken line shows the median model spectrum simulated as described in the text, and the thinner blue lines represent the 68 credible bands. The black line is the data spectrum.

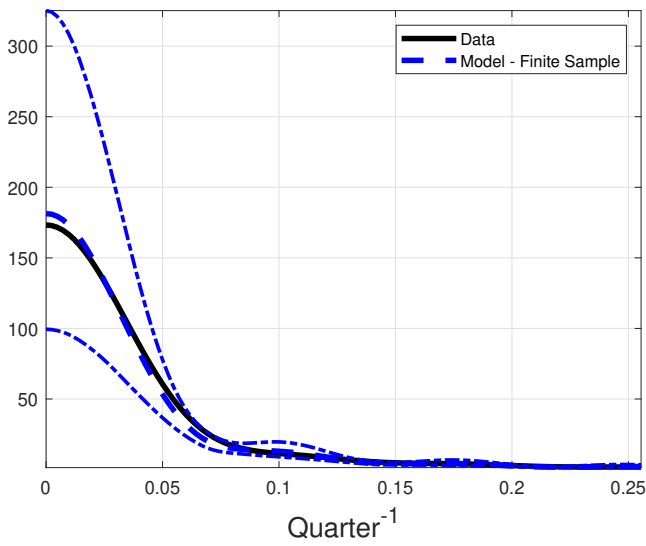
main conclusion, as only the endogenous growth model accurately tracks the empirical spectrum.¹ We also tried if results change when we use measurement error in the observed RER instead of the UIP shock. This serves as another check, if having potentially persistent UIP shocks drives our main conclusions. Figure 24 shows that, while the overall fit clearly deteriorates, our conclusion that endogenous productivity helps explain RER dynamics remains true.

To keep data and model comparable, we simulated finite samples of the same length as the data. Figure 25 simulates one sample of a 100,000 quarters, approaching the ergodic spectrum for both models. Because in long samples it is more likely to observe persistent low-frequencies fluctuations, the spectra are higher for both models. Nevertheless, the exogenous growth model still lies far from the empirical counterpart. It is also interesting to note that our model implies that the “true” long-run persistence of the RER is even higher than the data. Taking the results from the last few experiments together, we conclude that the dominance of the endogenous growth model does not depend on our simulation choices but rather on the internal propagation of the model.

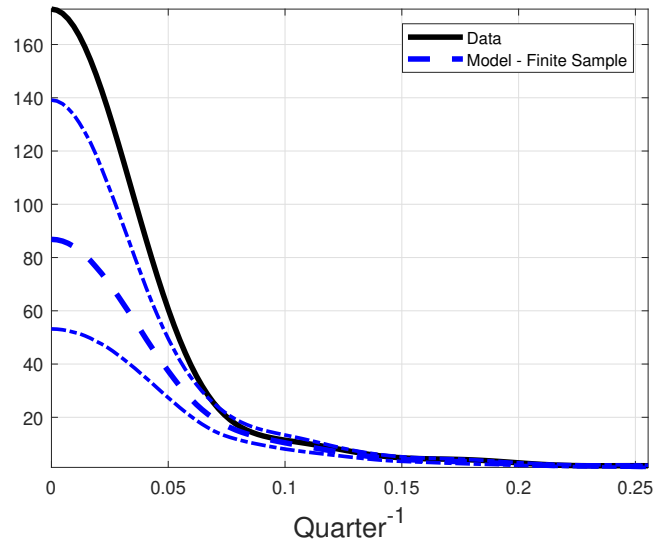
Finally, one might wonder if including the period after 2007, when monetary policy was constrained by the effective lower bound in many economies in our sample, matters for our results, as this could cause a structural break. To analyze this possibility, we drop all observations after 2007 from our estimation.² We also shorten the time series for the construction of the RER spectra accordingly. While we see significant changes in some estimated parameters, Figure 26 demonstrates that our key result is robust to using only data from before 2008.

¹In each simulation we draw 1179 periods and discard the first 1000 to randomize the initial conditions as well.

²We thank an anonymous referee for suggesting this experiment.



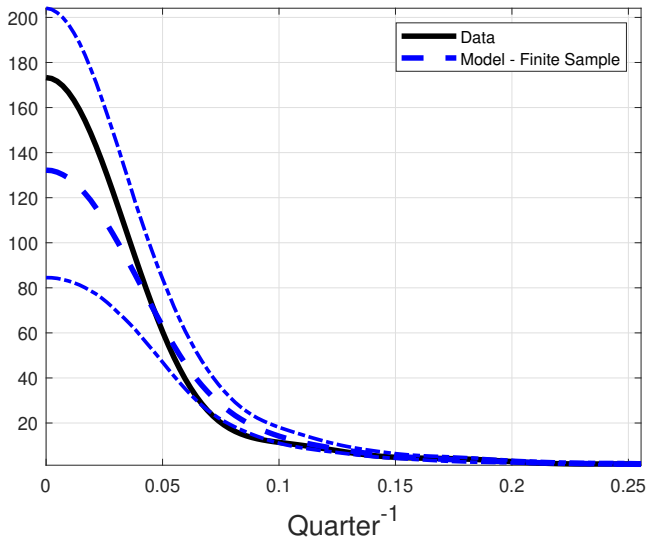
(a) Endogenous Growth



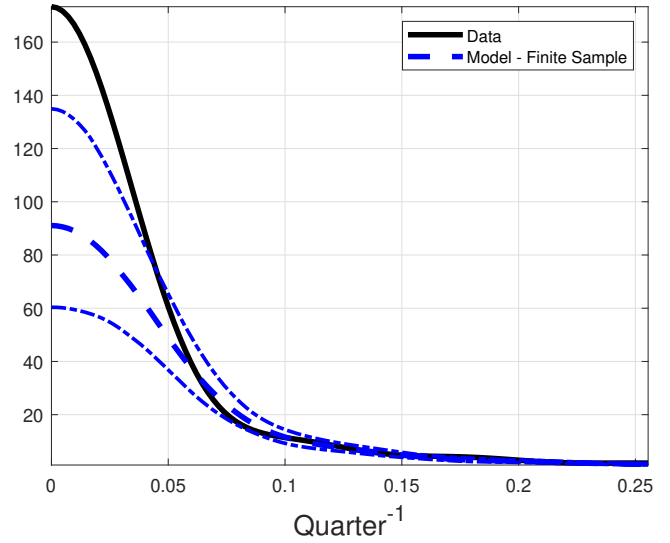
(b) Exogenous Growth

Figure 23: Robustness – I.I.D. Normal Shocks

Notes: The thick blue broken line shows the median model spectrum simulated as described in the text and the thinner blue lines represent the 68 percent bands from the simulations. The black line is the data spectrum.



(a) Endogenous Growth

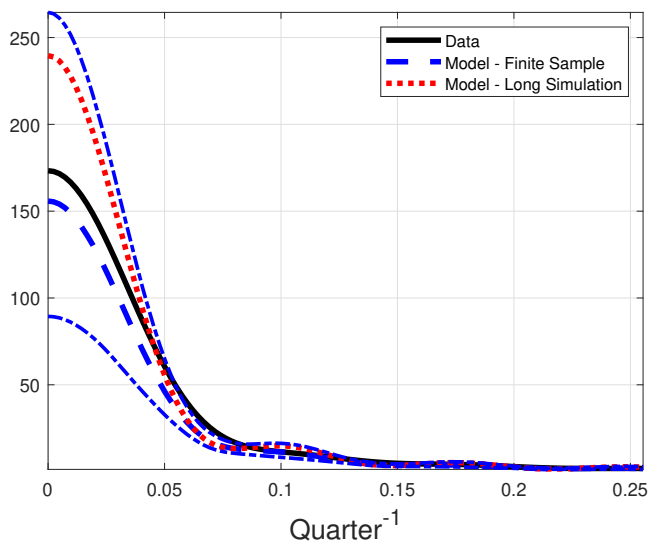


(b) Exogenous Growth

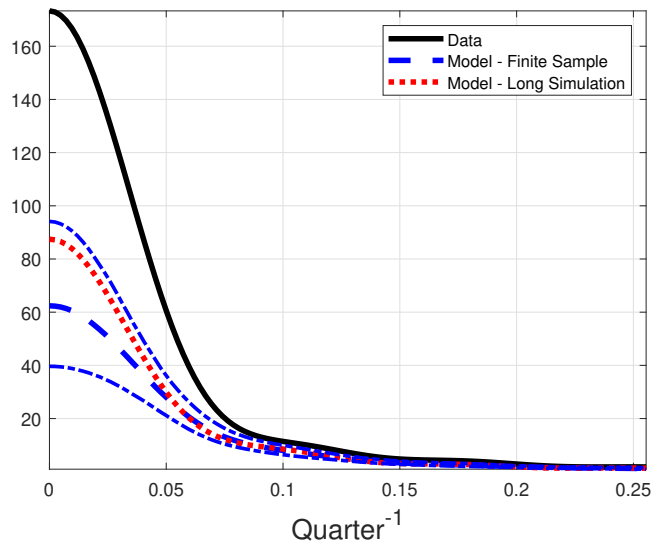
Figure 24: Measurement Error

Notes: The thick blue broken line shows the median model spectrum simulated as described in the text, and the blue thinner lines represent the 68 percent bands from the simulations. The black line is the data spectrum.

Table 12 shows the variance decomposition for the RER at business cycle and low frequency.



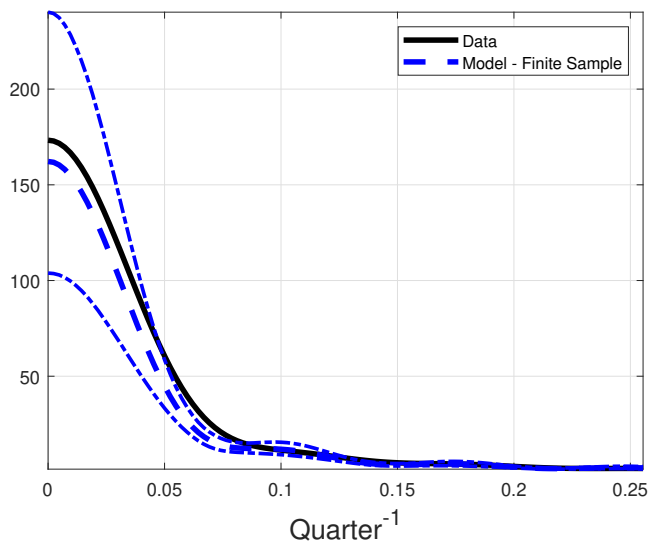
(a) Endogenous Growth



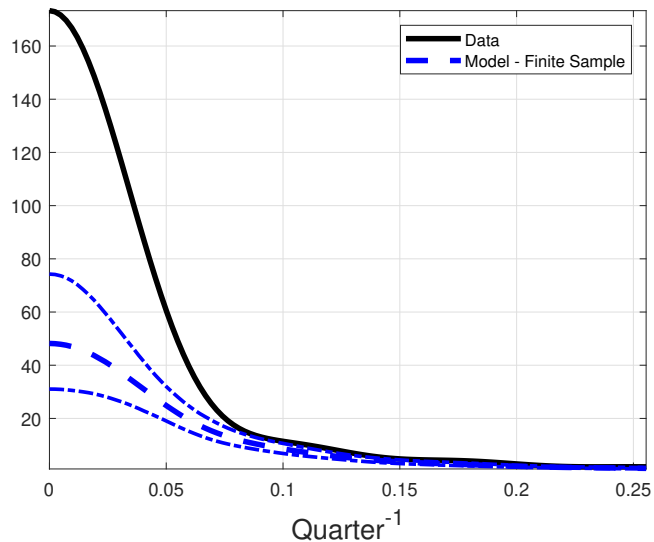
(b) Exogenous Growth

Figure 25: Robustness – Role of Simulation Length

Notes: The red dotted line shows the spectrum constructed from a 100000 period simulation of the RER in the respective models. The thick blue broken line shows the median model spectrum simulated as described in the text, and the thinner blue lines represent the 68 percent bands from the simulations. The black line is the data spectrum.



(a) Endogenous Growth



(b) Exogenous Growth

Figure 26: Pre-2008 Sample

Notes: The thick blue broken line shows the median model spectrum simulated as described in the text, and the thinner blue lines represent the 68 percent bands from the simulations. The black line is the data spectrum.

Table 12: Variance Decomposition - RER - Business Cycle and Low Frequency

	ψ	ψ^*	g	g^*	Z	Z^*	q	q^*	ζ	ζ^*	Ω^g	Ω^f	β	β^*	U
Endo-All	1.28	0.44	0.77	0.35	0.80	2.31	5.82	0.62	21.21	2.54	0.00	16.15	0.30	0.13	47.29
Endo-BC	0.43	0.17	0.29	0.15	0.36	0.31	16.78	5.04	0.30	0.07	0.00	1.67	0.14	0.08	74.22
Endo-Low	1.35	0.46	0.81	0.38	0.84	2.43	4.69	0.17	23.38	2.74	0.00	17.76	0.31	0.13	44.53
Exo-All	5.29	1.68	1.53	0.76	3.35	4.58	4.64	1.49	0.00	0.00	0.00	15.76	9.91	0.79	50.22
Exo-BC	2.85	1.37	1.12	0.64	4.15	2.44	12.92	3.98	0.00	0.00	0.00	0.79	2.30	0.78	66.66
Exo-Low	6.26	1.80	1.67	0.81	3.04	5.40	1.37	0.49	0.00	0.00	0.00	21.68	13.08	0.81	43.59

Notes: This table lists the variance decomposition for selected variables from the endogenous growth model (“Endo”) and the exogenous growth model (“Exo”) from a long simulation of 25000 periods with 1000 periods burn-in. It displays the standard variance decomposition (“All”) as well as the variance decomposition at business cycle frequency (“BC”)—obtained using the bandpass filter for 2-32 quarters—and at low frequencies (“Low”) obtained as the residual.

E Online Appendix: IRFs to UIP and Trade Shock

This appendix shows the IRFs to a UIP and relative trade shock in the full estimated endogenous and exogenous growth models.

Figure 27 compares the response of the home country—under endogenous and exogenous growth—to a favorable UIP shock. The favorable UIP shock decreases the cost of borrowing for the domestic economy, appreciating the exchange rate. As a result of a lower cost of borrowing from abroad, the local interest rate falls, impacting R&D and investment. R&D expenditures increase due to higher demand and, therefore, higher profits associated with domestic production. The lingering expansion helps the domestic country repay the borrowed funds without reducing consumption or investment. In addition, the lower domestic interest rate increases the present value of future profits, providing further incentive to R&D investment. As a result, the expansion of R&D triggers the short- and medium-run mechanisms described in the main text. Not surprisingly, the responses of every real variable are amplified on impact and are significantly more persistent in the endogenous growth economy. Relative to the exogenous growth model (dotted red lines), the endogenous version delivers far more persistent changes in economic activity, resulting in the lower-frequency movements in the RER. Two features of the UIP shock worth stressing are (1) it generates effortlessly co-movement in the domestic economy and (2) it induces a hump-shaped response of the RER. The second feature is crucial to induce a realistic half-life.

Figure 28 shows the IRFs to a relative trade shock (Ω_t^l). In both models, this shock decreases the cost of exporting from the home economy, making home goods cheaper in the foreign country and, therefore, resulting in a depreciation of the exchange rate. The simultaneous increase in the cost of selling the foreign good to the home economy boosts this effect. Under endogenous growth, the favorable trade shock increases the demand for exports, triggering an increase in the demand for home intermediate goods. This increase in demand translates into higher profits that provide incentives for R&D investment, which, once again, triggers the short-run wealth effects and medium-run productivity dynamics described in Figure 13. Therefore, the endogenous growth model amplifies the short-run responses and produces rich and persistent dynamics in response to the main shocks that drive the exchange rate.

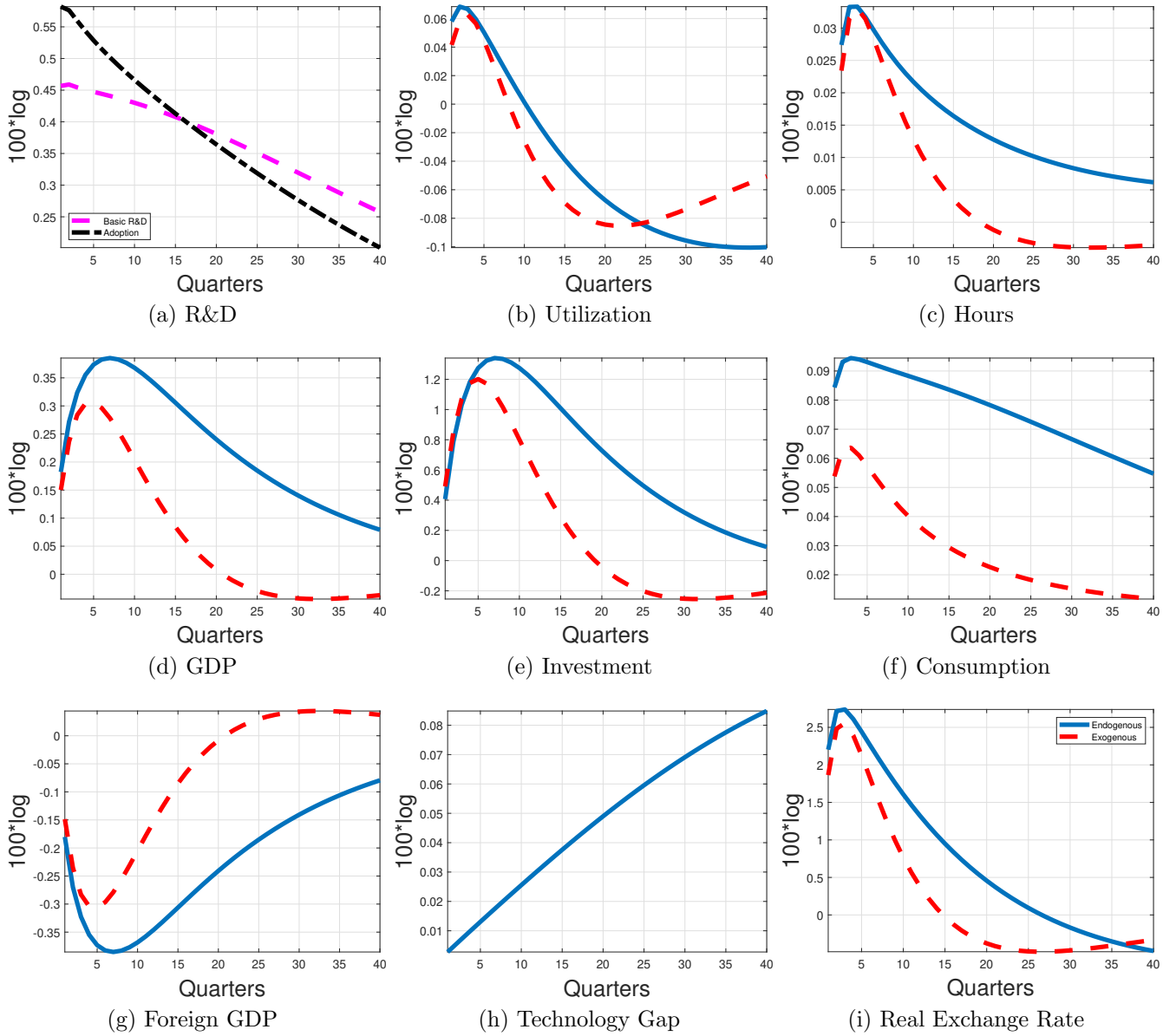


Figure 27: Impulse Response Functions to UIP Shock

Notes: The figure shows the IRFs from the endogenous growth model in blue solid lines relative to the model path before the shock. The red dotted lines show the same for the exogenous growth model. In the upper-left quadrant, the dynamics of basic research and development and adoption are shown as black and magenta broken lines, respectively.

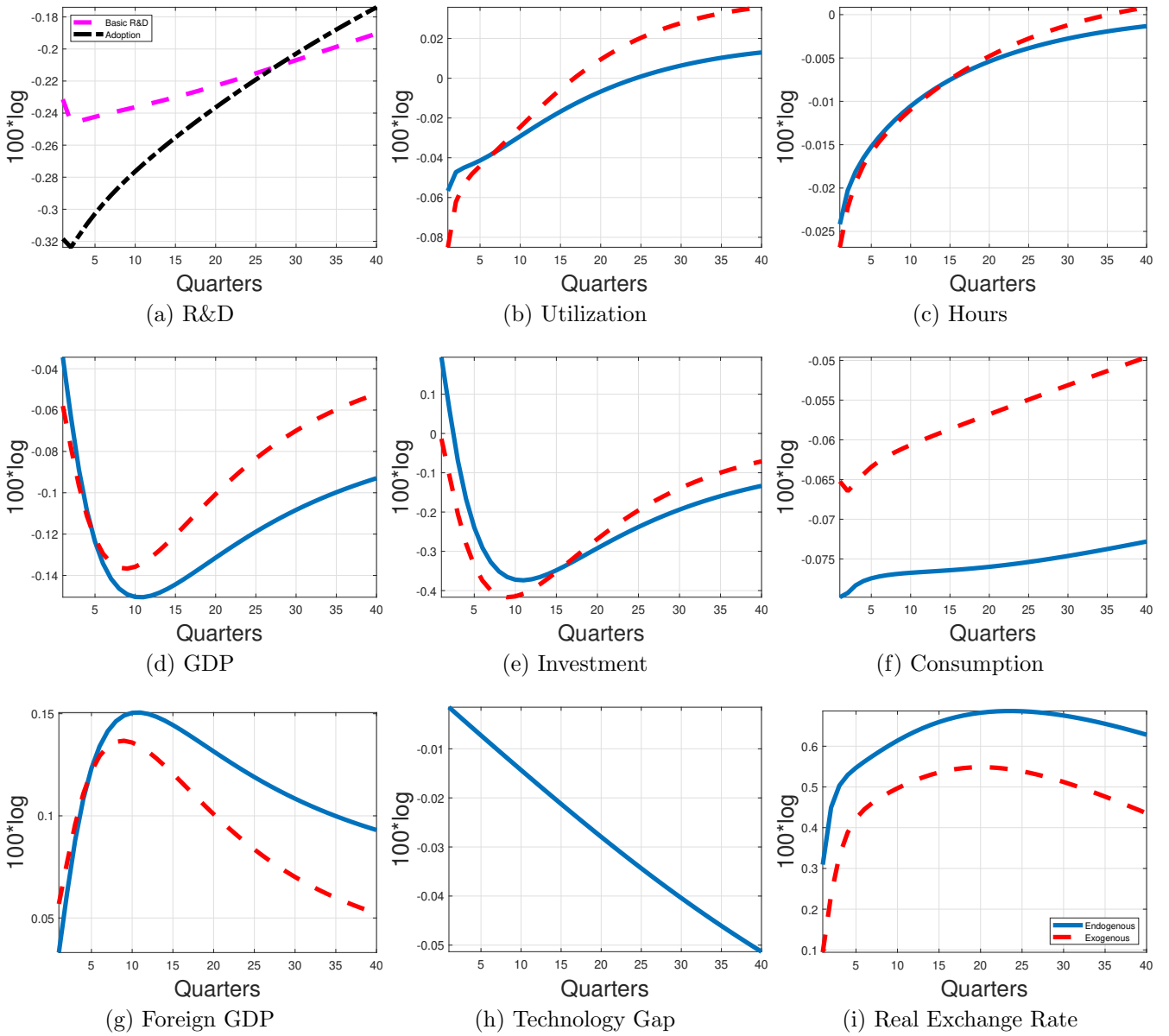


Figure 28: Impulse Response Functions to a Relative Trade Cost Shock

Notes: The figure shows the IRFs from the endogenous growth model in blue solid lines relative to the model path before the shock. The red dotted lines show the same for the exogenous growth model. In the upper-left quadrant, the dynamics of basic research and development and adoption are shown as black and magenta broken lines, respectively.

F Online Appendix: IRFs to Preference and TFP Shock – Simple Model

This appendix shows the IRFs to domestic preference and TFP shocks in the four versions of the simple model discussed in the main text. They are displayed in Figures 29 and 30, respectively. First, we show them for the estimated simple endogenous growth model and the estimated simple exogenous growth model. In addition, we show the IRFs from the simple exogenous growth model with the estimated parameters from the endogenous growth model to demonstrate that this difference in parameters only explains a small share of the difference between the two models. Finally, we re-estimate the endogenous growth model with a lower calibrated R&D elasticity – we set η to 0.25, half the value that we assume for the other variant. We can see that this modification matters for the quantitative dynamics, so the time series data are likely to be informative about this parameter when moving to the estimation of the full model.

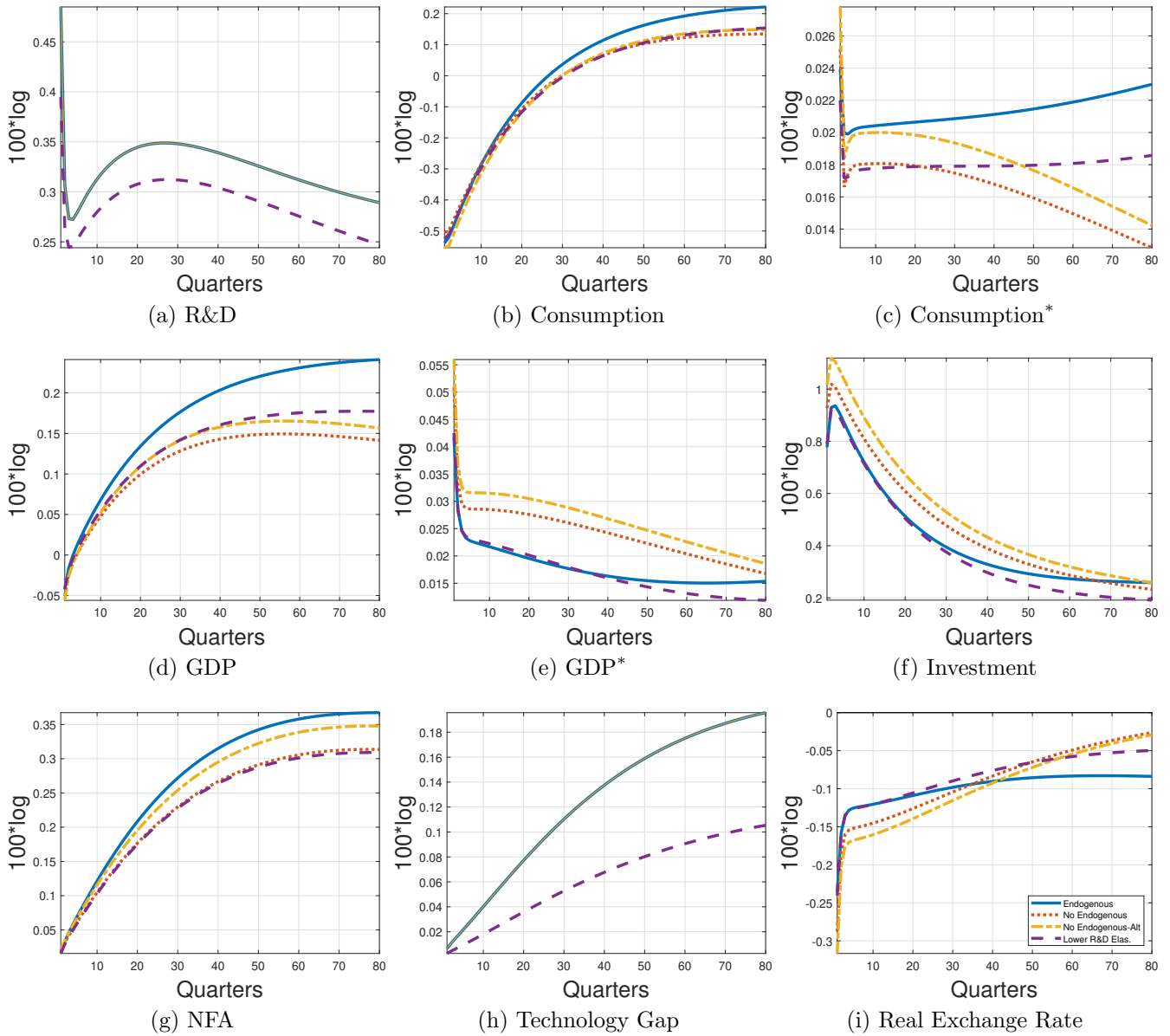


Figure 29: IRF Preference Shock – Simple Model

Notes: The figure shows the IRFs to a preference shock in country one from variations of the simple model as discussed in the main text.

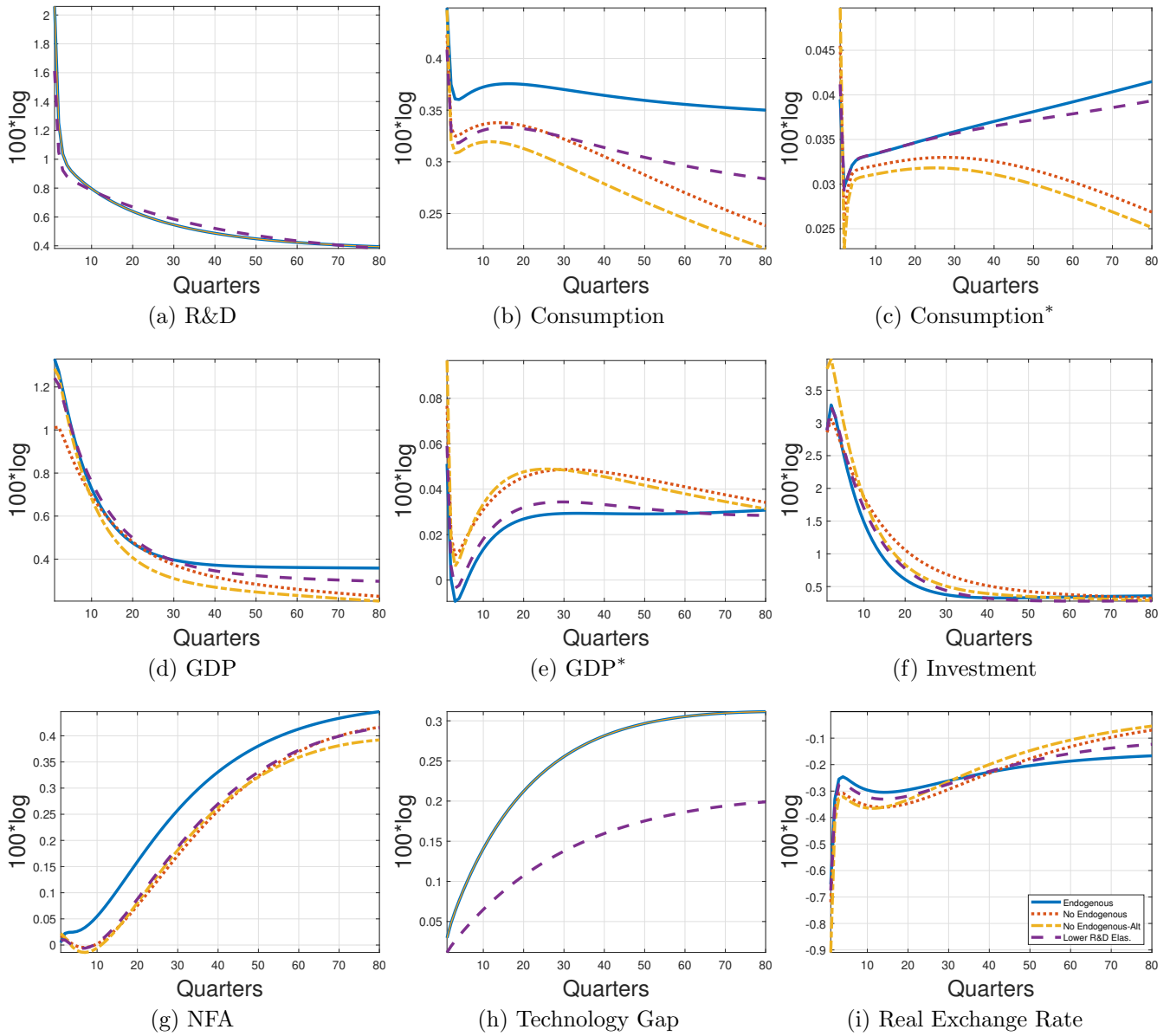


Figure 30: IRF TFP Shock – Simple Model

Notes: The figure shows the IRFs to a TFP shock in country one from variations of the simple model as discussed in the main text.

G Productivity Shocks and Exchange Rate Appreciations

In this appendix, we study the co-movement between productivity and the RER. [Corsetti et al. \(2006\)](#) and [Corsetti et al. \(2014\)](#) use VARs with long-run and sign restrictions, respectively, to study this co-movement. Both studies show that a rise in labor productivity in the tradable sector in a developed country, relative to its main trading partners, coincides with an appreciation of the RER. While our model lacks the distinction between the tradable and non-tradable sector, we can still study the co-movement between labor productivity and RER in our setup. TFP shocks in the model lead to a rise in relative labor productivity and a depreciation of the RER. However, the Solow residual moves in the model not only because of TFP shocks, but also triggered by endogenous changes in productivity through R&D, variable factor utilization, and fixed costs in production. Therefore, inspired by [Corsetti et al. \(2014\)](#), we estimate a VAR on model simulated data and “identify supply shocks” using sign restrictions to study the co-movement between productivity and the RER.

In particular, we simulate 10,000 data samples from our endogenous growth model, each of length 180 quarters. We then estimate a VAR with four lags on each sample, which includes the logged cross-country differences in labor productivity, GDP, and consumption, as well as the RER. We identify supply shocks from each of these VARs through sign restrictions, imposing that a supply shock has to raise relative labor productivity and GDP above zero on impact and for all 20 quarters after the shock. We borrow these restrictions from [Corsetti et al. \(2014\)](#) but impose them on the whole economy instead of the tradable sector.³ We draw 100 such shocks for each VAR. Results are robust to the number of draws and the number of VARs as well as the exact length of periods we impose the sign restriction to hold as well as the lag length of the VAR. Pooling the draws across the VARs, we construct IRFs using the median and 32-68 point-wise confidence bands. Results are shown in [Figure 31](#).

The identified supply shock leads to a significant rise in labor productivity (LP), GDP, and consumption for country 1 relative to country 2. The shock triggers a significant appreciation of the RER lasting for at least 2 years. An econometrician might, therefore, conclude that a supply shock causes an appreciation of the RER. Part of this result is likely driven by demand shocks in the model moving measured productivity and the RER together. In fact, our one sector economy cannot allow for all the important intricacies of the multi-sector identification in [Corsetti et al. \(2014\)](#). To alleviate this concern, we repeat the above experiment simulating the structural model only with shocks that affect supply directly by changing the production possibility frontier of the economy. This variation focuses exclusively on the type of shocks that [Corsetti et al. \(2014\)](#) aim to capture. As [Figure 32](#) shows, the RER still appreciates on impact, albeit less and with less persistence. To interpret the possibility of an appreciation despite rising productivity after a supply shock, it is worth remembering that rising incentives to perform R&D tend to lead initially to both an increase in productivity

³The absence of the tradable sector also implies that we cannot impose restrictions on sectoral labor productivity differences and prices. While this might weaken the ability of the VAR to differentiate among shocks, we chose to stay within the realm of our structural model and leave a further analysis to future work.

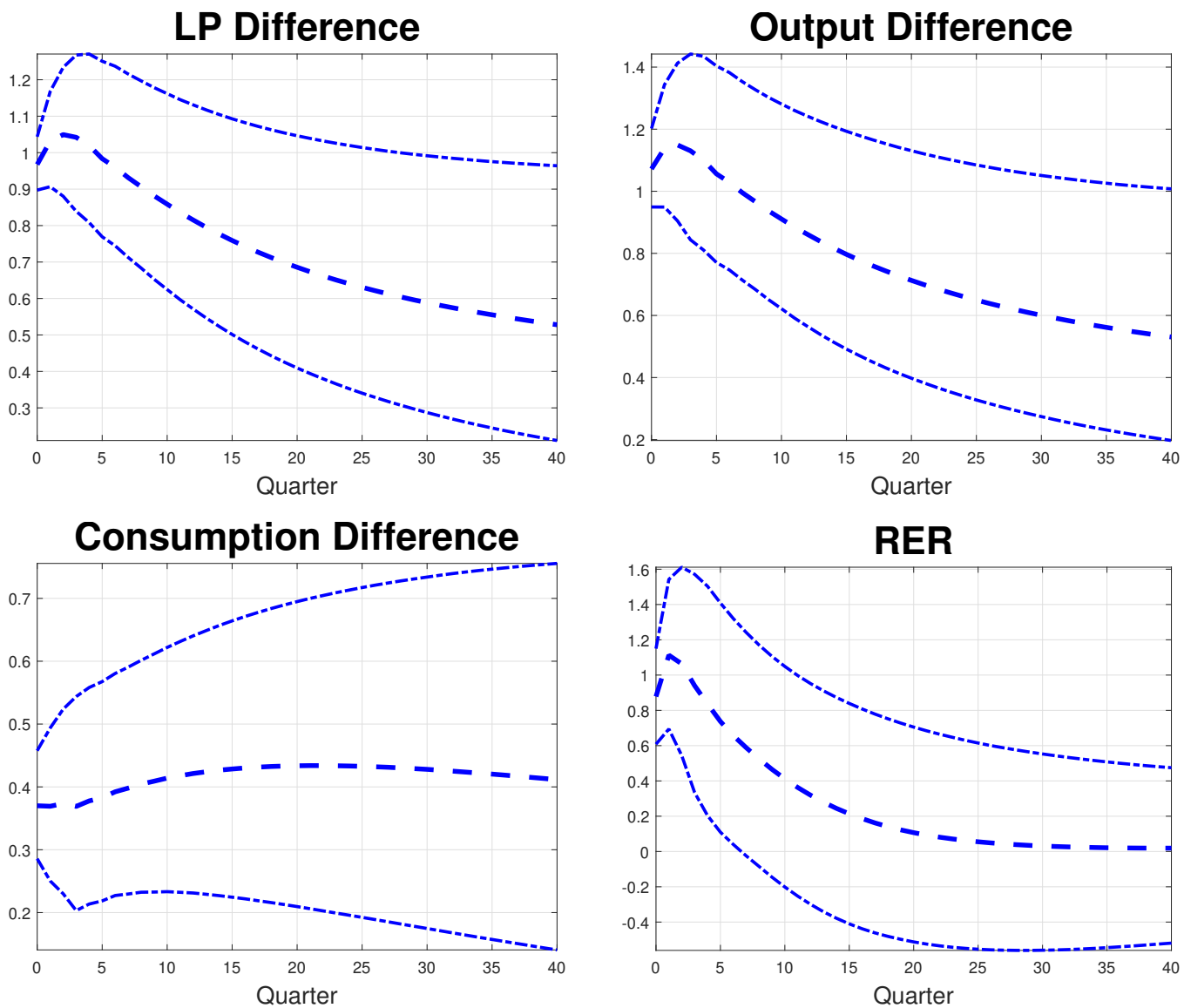


Figure 31: Sign Restriction VAR

Notes: The thick, blue, broken line shows the median response, and the thinner blue lines represent the 68 percent confidence intervals.

and an appreciation (see Figure 13 for the case of the R&D shock).

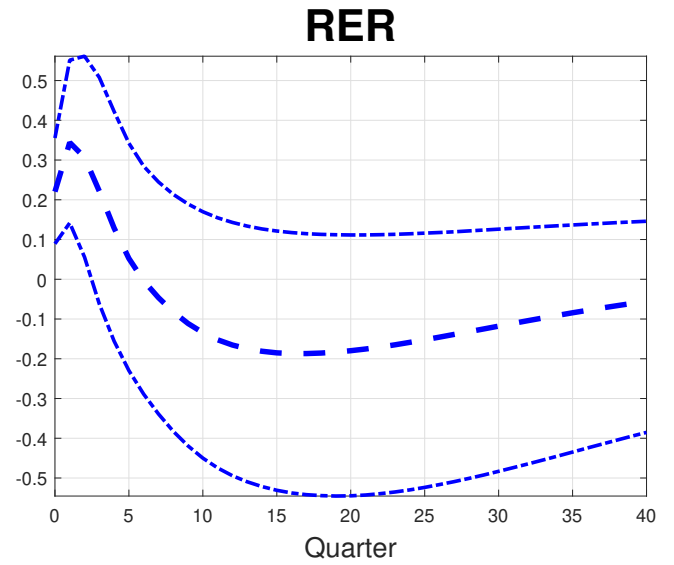
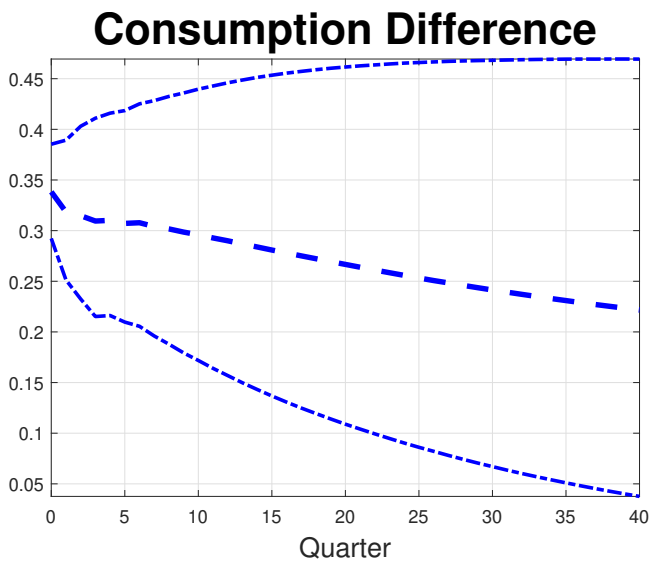
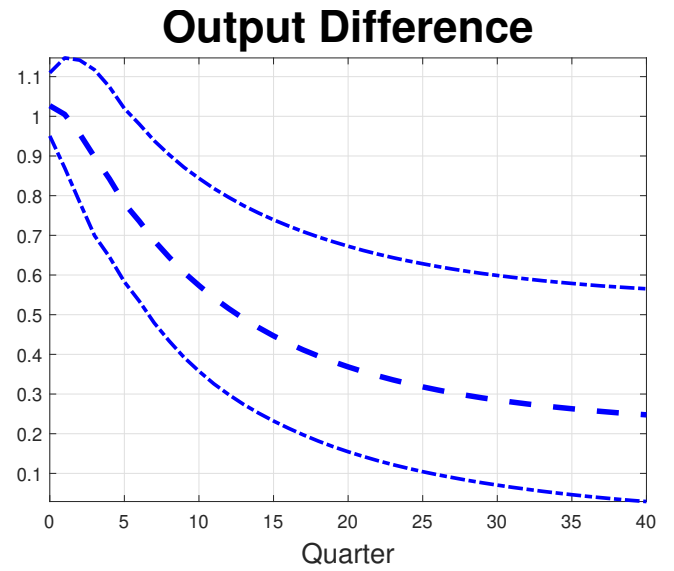
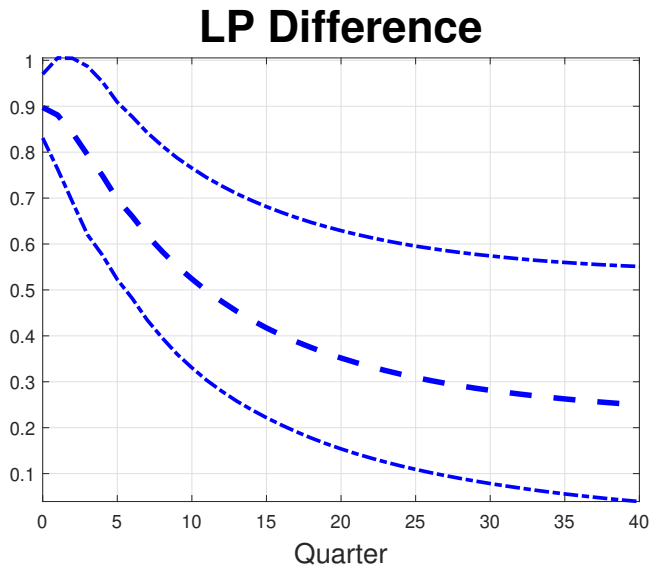


Figure 32: Sign Restriction VAR - Supply Shocks Only

Notes: The thick, blue, broken line shows the median response, and the thinner blue lines represent the 68 percent confidence intervals.

H Online Appendix: Model Equations for Full Model

H.1 Market Clearing

In this subsection, we collect the market clearing conditions omitted from the main text:

$$Y_t = C_t + I_t + S_t + (N_{t-1} - A_{t-1})a_t + A_{t-1}m_t + G_t Y_t + \Phi A_{t-1}$$

International bond demand and supply have to be in equilibrium:

$$b_t + b_t^* = 0.$$

In addition, international goods market clearing requires:

$$P_t^* b_t = p_{I,t}^* y_{I,t}^* - p_{I,t} y_{I,t} + P_t^* R_{t-1}^* b_{t-1}.$$

Factor market clearing requires

$$\bar{K}_{D,t} + \bar{K}_{I,t} = k_{t-1} u_t$$

$$L_{D,t} + L_{I,t} = l_t$$

$$m_{D,t} + m_{I,t} = m_t.$$

Profits paid to the household equal the profits from the intermediate good producer net of adoption and R&D expenditures:

$$\Pi_t = A_{t-1} \pi_t - S_t - (N_{t-1} - A_{t-1}) a_t$$

H.2 Characterization

In this subsection, we collect the equations characterizing an equilibrium. To keep things brief we drop the equations for stochastic processes and the foreign economy, the latter being essentially duplicates of the equations for the domestic economy. In the following equations ν_t^x with x a letter are Lagrange multipliers.

$$\prod_{s=0}^{t-1} \beta_s \left(c_t - \psi_{1,t} x_t l_t^{1+\psi_2} \right)^{-\sigma} - \nu_t^c P_t = 0$$

$$- \prod_{s=0}^{t-1} \beta_s \left(c_t - \psi_{1,t} x_t l_t^{1+\psi_2} \right)^{-\sigma} \psi_{1,t} (1 + \psi_2) x_t l_t^{\psi_2} + \nu_t^c W_t P_t = 0$$

$$\nu_t^c P_t R_t^k k_{t-1} - \nu_t^k \delta'_k(u_t) k_{t-1} = 0$$

$$-P_t \nu_t^c + \nu_t^k q_t \left(1 - \phi_i \left(\frac{i_t}{i_{t-1}} \right) - \phi'_i \left(\frac{i_t}{i_{t-1}} \right) \frac{i_t}{i_{t-1}} \right) + q_{t+1} \nu_{t+1}^k \phi'_i \left(\frac{i_{t+1}}{i_t} \right) \frac{i_{t+1}^2}{i_t^2} = 0$$

$$-\nu_t^k + \nu_{t+1}^k (1 - \delta_k(u_t)) + \nu_{t+1}^c P_{t+1} R_{t+1}^k u_{t+1} = 0$$

$$-\nu_t^c P_t + \nu_{t+1}^c R_t P_{t+1} = 0$$

$$-\nu_t^c P_t^* + \nu_{t+1}^c R_t^* P_{t+1}^* \exp(U_t) \exp \left(\frac{\bar{b}_{t-1}}{A_{t-1}} \right)^{-\phi_1} \left(\frac{R_t R_{t-1}}{\mathbb{E}_t R_t R_{t+1}} \right)^{-\phi_2} = 0$$

$$k_t = (1 - \delta_k(u_t)) k_{t-1} + q_t \left(1 - \phi_i \left(\frac{i_t}{i_{t-1}} \right) \right) i_t$$

$$x_t = \bar{c}_t^\gamma x_{t-1}^{1-\gamma}$$

$$\beta^t \nu_t^c (P_t Y_t^{1-\rho} a_D y_{D,t}^{\rho-1} - p_{D,t}) + \psi_t \left(-\iota \left(\frac{\frac{y_{I,t}}{y_{D,t}}}{\frac{y_{I,t-1}}{y_{D,t-1}}} - 1 \right) \frac{-\frac{y_{I,t}}{y_{D,t}^2}}{\frac{y_{I,t-1}}{y_{D,t-1}}} \right) + \psi_{t+1} \left(-\iota \left(\frac{\frac{y_{I,t+1}}{y_{D,t+1}}}{\frac{y_{I,t}}{y_{D,t}}} - 1 \right) \frac{\frac{y_{I,t+1}}{y_{D,t+1}}}{y_{I,t}} \right) = 0$$

$$\beta^t \nu_t^c (P_t Y_t^{1-\rho} a_I \phi_t^\rho y_{I,t}^{\rho-1} - p_{I,t}) + \psi_t \left(-\iota \left(\frac{\frac{y_{I,t}}{y_{D,t}}}{\frac{y_{I,t-1}}{y_{D,t-1}}} - 1 \right) \frac{\frac{1}{y_{D,t}}}{\frac{y_{I,t-1}}{y_{D,t-1}}} \right) + \psi_{t+1} \left(-\iota \left(\frac{\frac{y_{I,t+1}}{y_{D,t+1}}}{\frac{y_{I,t}}{y_{D,t}}} - 1 \right) \frac{\frac{y_{I,t+1}}{y_{D,t+1}}}{-\frac{y_{I,t}}{y_{D,t}^2}} \right) = 0$$

$$\beta^t \nu_t^c P_t Y_t^{1-\rho} a_I \phi_t^{\rho-1} y_{I,t}^\rho - \psi_t = 0$$

$$Y_t = (a_D y_{D,t}^\rho + a_I (\phi_t y_{I,t})^\rho)^{\frac{1}{\rho}}$$

$$\phi_t = 1 - \frac{\iota}{2} \left(\frac{\frac{y_{I,t}}{y_{D,t}}}{\frac{y_{I,t-1}}{y_{D,t-1}}} - 1 \right)^2$$

$$y_t = Z_t \bar{K}_t^{\alpha_K} L_t^{\alpha_L} M_t^{\alpha_M}$$

$$M_t = A_{t-1}^{\frac{1}{\mu}} m_t$$

$$p_{D,t}\alpha_L \frac{y_t}{L_t} = P_t W_t$$

$$p_{D,t}\alpha_K \frac{y_t}{K_t} = P_t R_t^k$$

$$p_{D,t}\alpha_M \frac{y_t}{M_t} (A_{t-1} m_t^\mu)^{\frac{1}{\mu}-1} m_t^{\mu-1} = p_t$$

$$p_{D,t}\Omega_t^g \Omega_t^l = p_{I,t}^*$$

$$\frac{1}{\mu} P_t = p_t$$

$$\pi_t = \left(\frac{1}{\mu} - 1 \right) P_t m_t - \Phi$$

$$H_t = \pi_t + (1 - \delta_a) \Lambda_{t,t+1} H_{t+1}$$

$$\Lambda_{t,t+1} = \frac{\nu_{t+1}^c}{\nu_t^c}$$

$$N_t = (1 - \delta_n) N_{t-1} + \gamma_t$$

$$\gamma_t = \zeta \frac{(N_{t-1} + \tau N_{t-1}^*)^{1-\eta}}{S_t^{1-\eta}} S_t$$

$$\zeta \frac{(N_{t-1} + \tau N_{t-1}^*)^{1-\eta}}{S_t^{1-\eta}} \Lambda_{t,t+1} J_{t+1} = P_t$$

$$A_t = (1 - \delta_a) A_{t-1} + \lambda_t(a_t) (N_{t-1} - A_{t-1})$$

$$J_t = -P_t a_t + \Lambda_{t,t+1} (\lambda_t(a_t) H_{t+1} + (1 - \lambda_t(a_t)) (1 - \delta_n) J_{t+1})$$

$$P_t = \Lambda_{t,t+1} (\lambda_t'(a_t) H_{t+1} - \lambda_t'(a_t) (1 - \delta_n) J_{t+1})$$

$$\lambda_t(a_t) = \kappa_\lambda (a_t)^{\mu_\lambda}$$

$$Y_t = c_t + i_t + S_t + (N_{t-1} - A_{t-1})a_t + A_{t-1}m_t + G_t Y_t + \Phi A_{t-1}$$

$$b_t + b_t^* = 0$$

$$P_t^* b_t = p_{I,t}^* y_{I,t}^* - p_{I,t} y_{I,t} + P_t^* R_{t-1}^* b_{t-1}$$

$$y_t = y_{D,t} + y_{I,t}^* \theta^G \theta^R$$

$$L_t = l_t$$

$$\bar{K}_t = k_{t-1} u_t$$

H.3 Re-arrange and Normalize

Using the equations from the previous subsection of the appendix, we normalize the model by its stochastic trend to derive a stationary representation. We also simplify the equations slightly. The resulting equations were used to solve the model.

- $\tilde{\nu}_t^c = \frac{\nu_t^c}{\prod_{s=0}^{t-1} \beta_s A_{t-1}^{-\sigma}} P_t$
- $\tilde{c}_t = \frac{c_t}{A_{t-1}}$
- $\tilde{x}_t = \frac{x_t}{A_{t-1}}$
- $\tilde{A}_t = \frac{A_t}{A_{t-1}}$
- $\tilde{W}_t = \frac{W_t}{A_{t-1}}$
- $\tilde{\nu}_t^k = \frac{\nu_t^k}{\prod_{s=0}^{t-1} \beta_s A_{t-1}^{-\sigma}}$
- $RER_t = \frac{P_t}{P_t^*}$
- $\tilde{q}_t = \frac{q_t}{P_t}$
- $\tilde{p}_t = \frac{p_t}{P_t}$
- $\tilde{p}_t^* = \frac{p_t^*}{P_t^*}$
- $\tilde{k}_{t-1} = \frac{k_{t-1}}{A_{t-1}}$
- $\tilde{K}_t = \frac{\tilde{K}_t}{A_{t-1}}$
- $\tilde{i}_t = \frac{i_t}{A_{t-1}}$
- $\tilde{Y}_t = \frac{Y_t}{A_{t-1}}$
- $\tilde{y}_t = \frac{y_t}{A_{t-1}}$
- $\tilde{a}_t = \frac{a_t}{A_{t-1}}$
- $\tilde{\pi}_t = \frac{\pi_t P_t}{A_{t-1}}$
- $\tilde{S}_t = \frac{S_t}{A_{t-1}}$
- $\tilde{\gamma}_t = \frac{\gamma_t}{A_{t-1}}$
- $\tilde{N}_t = \frac{N_t}{A_{t-1}}$
- $\tilde{B}_t = \frac{B_t}{A_{t-1}}$

- $\tilde{M}_t = \frac{M_t}{A_{t-1}^\mu}$
- $\tilde{y}_{D,t} = \frac{y_{D,t}}{A_{t-1}}$
- $\tilde{y}_{I,t} = \frac{y_{I,t}}{A_{t-1}^*}$
- $\Gamma_{t-1} = \frac{A_{t-1}^*}{A_{t-1}}$
- $\tilde{H}_t = \frac{H_t}{P_t}$
- $\tilde{J}_t = \frac{J_t}{P_t}$
- $\tilde{b}_{D,t} = \frac{b_{D,t}}{A_{t-1}}$
- $\tilde{b}_{I,t} = \frac{b_{I,t}}{A_{t-1}^*}$

$$\left(\tilde{c}_t - \psi_{1,t}\tilde{x}_t L_t^{1+\psi_2}\right)^{-\sigma} - \tilde{\nu}_t^c = 0$$

$$-\left(\tilde{c}_t - \psi_{1,t}\tilde{x}_t L_t^{1+\psi_2}\right)^{-\sigma} \psi_{1,t}(1 + \psi_2)\tilde{x}_t L_t^{\psi_2} + \tilde{\nu}_t^c \tilde{W}_t = 0$$

$$\tilde{\nu}_t^c R_t^k - \delta'_k(u_t)\tilde{\nu}_t^k = 0$$

$$-\tilde{\nu}_t^c + \tilde{\nu}_t^k q_t \left(1 - \phi_i \left(\frac{\tilde{A}_{t-1}\tilde{i}_t}{\tilde{i}_{t-1}}\right) - \phi'_i \left(\frac{\tilde{A}_{t-1}\tilde{i}_t}{\tilde{i}_{t-1}}\right) \frac{\tilde{A}_{t-1}\tilde{i}_t}{\tilde{i}_{t-1}}\right) + \beta_t \tilde{A}_t^{-\sigma} \tilde{\nu}_{t+1}^k q_{t+1} \phi'_i \left(\frac{\tilde{A}_t \tilde{i}_{t+1}}{\tilde{i}_t}\right) \left(\frac{\tilde{A}_t \tilde{i}_{t+1}}{\tilde{i}_t}\right)^2 = 0$$

$$-\tilde{\nu}_t^k + \tilde{A}_t^{-\sigma} \beta \tilde{\nu}_{t+1}^k (1 - \delta_k(u_t)) + \tilde{A}_t^{-\sigma} \beta_t \tilde{\nu}_{t+1}^c R_{t+1}^k u_{t+1} = 0$$

$$-\tilde{\nu}_t^c + \tilde{A}_t^{-\sigma} \beta_t \tilde{\nu}_{t+1}^c R_t = 0$$

$$-\frac{\tilde{\nu}_t^c}{RER_t} + \tilde{A}_t^{-\sigma} \beta_t \frac{\tilde{\nu}_{t+1}^c R_t^*}{RER_{t+1}} \exp(U_t) \exp(\tilde{b}_t)^{-\phi_1} \left(\frac{RER_{t-1}}{\mathbb{E}_t RER_{t+1}}\right)^{-\phi_2} = 0$$

$$\tilde{k}_t \tilde{A}_t = (1 - \delta_k(u_t))\tilde{k}_{t-1} + q_t \left(1 - \phi_i \left(\frac{\tilde{i}_t \tilde{A}_{t-1}}{\tilde{i}_{t-1}}\right)\right) \tilde{i}_t$$

$$\tilde{x}_t = \left(\frac{\tilde{c}_t}{\tilde{A}_{t-1}}\right)^\gamma \left(\frac{\tilde{x}_{t-1}}{A_{t-1}}\right)^{1-\gamma}$$

$$\tilde{Y}_t^{1-\rho} a_D \tilde{y}_{D,t}^{\rho-1} + \tilde{Y}_t^{1-\rho} a_I \phi_t^{\rho-1} \tilde{y}_{I,t}^\rho \hat{\phi}_t \frac{\frac{\tilde{y}_{I,t}}{\tilde{y}_{D,t}}}{\frac{\tilde{y}_{I,t-1}}{\tilde{y}_{D,t-1}}} \Gamma_{t-1}^{1+\rho} \Gamma_{t-2}^{-1} - \beta \tilde{A}_t^{-\sigma} \frac{\tilde{\nu}_{t+1}^c}{\tilde{\nu}_t^c} \tilde{Y}_{t+1}^{1-\rho} a_I \phi_{t+1}^{\rho-1} \tilde{y}_{I,t+1}^\rho \hat{\phi}_{t+1} \frac{\frac{\tilde{y}_{I,t+1}}{\tilde{y}_{D,t+1}}}{\frac{\tilde{y}_{I,t}}{\tilde{y}_{D,t}}} \Gamma_t^{-\rho} \tilde{A}_t^* = \tilde{p}_{D,t}$$

$$\begin{aligned} & \tilde{Y}_t^{1-\rho} a_I \phi_t^\rho (\tilde{y}_{I,t} \Gamma_{t-1})^{\rho-1} - \tilde{Y}_t^{1-\rho} a_I \phi_t^{\rho-1} \tilde{y}_{I,t}^\rho \hat{\phi}_t \frac{\frac{1}{\tilde{y}_{D,t}}}{\frac{\tilde{y}_{I,t-1}}{\tilde{y}_{D,t-1}}} \Gamma_{t-1}^{\rho-1} \frac{\tilde{A}_{t-1}^*}{\tilde{A}_{t-1}} \\ & + \beta \tilde{A}_t^{-\sigma} \frac{\tilde{\nu}_{t+1}^c}{\tilde{\nu}_t^c} \tilde{Y}_{t+1}^{1-\rho} a_I \phi_{t+1}^{\rho-1} \tilde{y}_{I,t+1}^\rho \hat{\phi}_{t+1} \frac{\frac{\tilde{y}_{I,t+1}}{\tilde{y}_{D,t+1}}}{\frac{\tilde{y}_{I,t}^2}{\tilde{y}_{D,t}}} \Gamma_t^\rho \tilde{A}_t^* \frac{1}{\Gamma_{t-1}} = \frac{\tilde{p}_{I,t}}{RER_t} \end{aligned}$$

$$\tilde{Y}_t = (a_D \tilde{y}_{D,t}^\rho + a_I (\phi_t \tilde{y}_{I,t} \Gamma_{t-1})^\rho)^{\frac{1}{\rho}}$$

$$\phi_t = 1 - \frac{\iota}{2} \left(\frac{\frac{\tilde{y}_{I,t}}{\tilde{y}_{D,t}} \frac{\tilde{A}_{t-1}^*}{\tilde{A}_{t-1}} - 1}{\frac{\tilde{y}_{I,t-1}}{\tilde{y}_{D,t-1}} \frac{\tilde{A}_{t-1}^*}{\tilde{A}_{t-1}}} \right)^2$$

$$\hat{\phi}_t = \iota \left(\frac{\frac{\tilde{y}_{I,t}}{\tilde{y}_{D,t}} \frac{\tilde{A}_{t-1}^*}{\tilde{A}_{t-1}} - 1}{\frac{\tilde{y}_{I,t-1}}{\tilde{y}_{D,t-1}} \frac{\tilde{A}_{t-1}^*}{\tilde{A}_{t-1}}} \right)$$

$$\tilde{y}_t = Z_t \tilde{K}_t^{\alpha_K} L_t^{\alpha_L} \tilde{M}_t^{\alpha_M}$$

$$\tilde{M}_t = m_t$$

$$\tilde{p}_{D,t} \alpha_L \frac{\tilde{y}_t}{L_t} = \tilde{W}_t$$

$$\tilde{p}_{D,t} \alpha_K \frac{\tilde{y}_t}{\tilde{K}_t} = R_t^k$$

$$\tilde{p}_{D,t} \alpha_M \tilde{y}_t \tilde{M}_t^{-\mu} \tilde{m}_t^{\mu-1} = \tilde{p}_t$$

$$\tilde{p}_{D,t} \theta^G \theta^R = \tilde{p}_{I,t}^*$$

$$\frac{1}{\mu} = \tilde{p}_t$$

$$\tilde{\pi}_t = \left(\frac{1}{\mu} - 1 \right) m_t - \Phi$$

$$\tilde{H}_t = \tilde{\pi}_t + (1 - \delta_a)\tilde{\Lambda}_{t,t+1}\tilde{H}_{t+1}$$

$$\tilde{\Lambda}_{t,t+1} = \beta_t \tilde{A}_t^{-\sigma} \frac{\tilde{v}_{t+1}^c}{\tilde{v}_t^c}$$

$$\tilde{A}_t \tilde{N}_t = (1 - \delta_n)\tilde{N}_{t-1} + \tilde{\gamma}_t$$

$$\tilde{\gamma}_t = \zeta \left(\frac{\tilde{N}_{t-1}}{\tilde{A}_{t-1}} + \tau \frac{\tilde{N}_{t-1}^* \Gamma_{t-1}}{\tilde{A}_{t-1}} \right)^{1-\eta} \tilde{S}_t^\eta$$

$$\frac{\zeta \left(\frac{\tilde{N}_{t-1}}{\tilde{A}_{t-1}} + \tau \frac{\tilde{N}_{t-1}^* \Gamma_{t-1}}{\tilde{A}_{t-1}} \right)^{1-\eta}}{\tilde{S}_t^{1-\eta}} \tilde{\Lambda}_{t,t+1} \tilde{J}_{t+1} = 1$$

$$\tilde{A}_t = (1 - \delta_a) + \lambda_t \left(\frac{\tilde{N}_{t-1}}{\tilde{A}_{t-1}} - 1 \right)$$

$$\tilde{J}_t = -a_t + \tilde{\Lambda}_{t,t+1} \left(\lambda_t(a_t) \tilde{H}_{t+1} + (1 - \lambda_t(a_t))(1 - \delta_n) \tilde{J}_{t+1} \right)$$

$$1 = \tilde{\Lambda}_{t,t+1} \left(\lambda'_t(a_t) \tilde{H}_{t+1} - \lambda'_t(a_t)(1 - \delta_n) \tilde{J}_{t+1} \right)$$

$$\lambda_t(a_t) = \kappa_\lambda (a_t)^{\mu_\lambda}$$

$$\tilde{Y}_t = \tilde{c}_t + \tilde{i}_t + \tilde{S}_t + \left(\frac{\tilde{N}_{t-1}}{\tilde{A}_{t-1}} - 1 \right) a_t + m_t + G_t \tilde{Y}_t + \Phi$$

$$\tilde{b}_t + \tilde{b}_t^* \Gamma_{t-1} = 0$$

$$\tilde{b}_t = RER_t \tilde{p}_{I,t}^* y_{I,t}^* - \tilde{p}_{I,t} \Gamma_{t-1} \tilde{y}_{I,t} + R_{t-1}^* \frac{\tilde{b}_{t-1}}{\tilde{A}_{t-1}}$$

$$\tilde{y}_t = \tilde{y}_{D,t} + \tilde{y}_{I,t}^* \theta^G \theta^R$$

$$\tilde{K}_t = \tilde{k}_{t-1} u_t$$

References

- Corsetti, Giancarlo, Luca Dedola, and Sylvain Leduc, “The international dimension of productivity and demand shocks in the US economy,” *Journal of the European Economic Association*, 2014, 12 (1), 153–176.
- , – , – , Susanto Basu, and Robert Kollmann, “Productivity, External Balance, and Exchange Rates: Evidence on the Transmission Mechanism among G7 Countries [with Comments],” in “NBER International Seminar on Macroeconomics,” Vol. 2006 The University of Chicago Press Chicago, IL 2006, pp. 117–194.